THIN ICE AREA EXTRACTION IN THE BERING SEA & THE GULF OF ST. LAWRENCE USING AMSR2 DATA

Kenta Miyao[1], Tomoko Kasuda[1], Kazuhiro Naoki[1] and Kohei Cho[1]
[1]Tokai University Research & Information Center (TRIC),
2-28-4, Tomigaya, Shibuya-k, Tokyo 151-0063, Japan,
Email: kohei.cho@tokai-u.jp

KEY WORDS: Sea ice, Passive microwave radiometer, GCOM-W, global warming

ABSTRACT: Sea ice has an important role of reflecting the solar radiation back into space. In addition, the heat flux of ice in thin ice areas is strongly affected by the ice thickness difference. Therefore, ice thickness is important parameter of sea ice. In the previous study, the authors have developed a thin ice area extraction algorithm using passive microwave radiometer AMSR2 for the Sea of Okhotsk. The basic idea of the algorithm is to use the brightness temperature scatter plots of AMSR2 19GHz polarization difference (V-H) vs 19GHz V polarization. In this study, the authors have applied the algorithm to the other seasonal sea ice zones in the Northern Hemisphere, i. e. the Bering Sea and the Gulf of St. Lawrence. As for the Bering Sea, the algorithm worked quite well without changing the parameters of the algorithm used for the Sea of Okhotsk. As for the Gulf of St. Lawrence, the initial result suggested that the algorithm is applicable with some modification of the parameters.

1. INTRODUCTION

Passive microwave radiometers onboard satellites can penetrate clouds and can monitor the global sea ice distribution on daily basis. The sea ice observation with passive microwave radiometer started in 1978 and has over 38 years record. The long term observation data showed clear decline trend of the Arctic sea ice cover (Comiso et al., 2008, Comiso, 2012) which is used as an evidence of global warming in the Fifth Assessment Report of IPCC (2014). The passive microwave radiometer AMSR2 onboard GCOM-W satellite was successfully launched by JAXA in May 2012. On 16 September 2012, the minimum sea ice extent in Northern Hemisphere was recorded by AMSR2 in the history of passive microwave sensor observation from space. The importance of sea ice monitoring from space is increasing. Ice concentration is the most fundamental parameter of sea ice which can be calculated from brightness temperatures measured by passive microwave radiometers. There are number of sea ice concentration algorithms including NASA Team Algorithm (Cavarieli et al., 1984) and Bootstrap Algorithm (Comiso, 1995). Sea ice extent and sea ice area can be calculated from the sea ice concentration data. Ice thickness is another important parameter of sea ice. However, the sea ice thickness information cannot be estimated from the sea ice concentration data. Studies on estimating ice thickness from the brightness temperature data acquired from passive microwave radiometers onboard satellites have been done in the past including those of Tateyama et al. (2002), Martin et al. (2005), and Tamura et al. (2007). However, the detailed validation of the accuracy of the estimated sea ice thickness is still on the way. Estimating ice thickness from passive microwave radiometer is not easy. Recently, the authors have developed a method to detect thin ice area using brightness temperature scatter plots of AMSR2 19GHz polarization difference (V-H) vs 19GHz V polarization (Cho et. Al, 2012, Tokutsu et. Al, 2014). The thin ice area extraction results were compared with simultaneously collected MODIS images for the Sea of Okhotsk for verification. It worked quite well in the Sea of Okhotsk. In this study, the authors have applied the algorithm to other seasonal sea ice zones in the Northern Hemisphere, i. e. the Bering Sea and the Gulf of St. Lawrence. The result is described in this paper.

2. TEST SITE

In this study, two seasonal sea ice zones in the Northern Hemisphere namely the Sea of Bering and the Gulf of St. Lawrence were selected as the test site for the evaluation of thin ice area extraction. Figure 1 show the maps of the test sites. The Bering Sea is located at the northernmost part of the Pacific Ocean, and connected to Arctic Ocean by the Bering Strait. The sea is surrounded by the Siberia, the Kamchatka Peninsula, the Alaska Peninsula and the Aleutian Islands. The Gulf of St. Lawrence is located at eastern Canada, connected to the Atlantic Ocean.

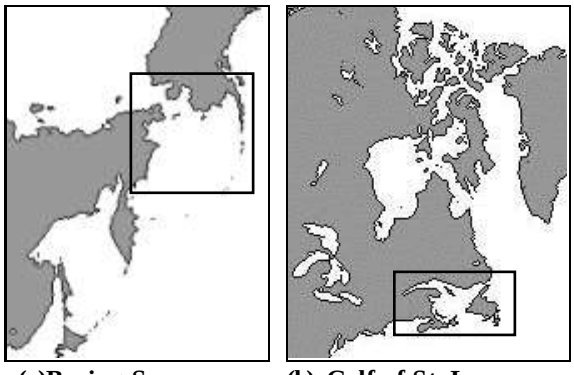

(a)Bering Sea **(b) Gulf of St. Lawrence**

Figure 1. Test Site

3. ANALYZED DATA

The brightness temperature data of passive microwave radiometer AMSR2 onboard GCOM-W satellite were used in this study. The ice concentration data derived from AMSR2 data using Bootstrap Algorithm is also used in this study. The diameter of the main reflector of AMSR2 is 2.0m, which is one of the largest size of reflector used for passive microwave radiometer is space. This means that IFOV of AMSR2 is higher than the other passive microwave radiometers. Table 1 shows the specifications of AMSR2. In addition, in order to identify thin ice areas, data collected by optical sensor MODIS onboard Aqua satellite were used as reference. Since Aqua and GCOM-W are in the same orbital "track" under the frame work of the NASA's A-Train, the constellation of satellites, MODIS onboard Aqua observed the same area four minutes after the observation of AMSR2 onboard GCOM-W. Therefore, MODIS data is one of the most effective validation data for AMSR2 data. Table 3 show the specifications of MODIS. As for MODIS, only the Band 1 and 2 which have the 250m resolution were used in this study.

Table 1. Specifications of AMSR2

Frequency (polarization)	IFOV	Swath	Incident angle
6.925GHz（V,H）	35×62 km	1450 km	55 deg
10.65GHz (V,H)	24×42 km		
18.7GHz（V,H）	14×22 km		
23.8GHz（V,H）	15×26 km		
36.5GHz（V,H）	7×12 km		
89.0GHz（V,H）	3×5 km		

Table 2. Specifications of MODIS

Band	Wavelength	IFOV	Swath
1	0.620-0.670 μm	250 m	2330 km
2	0.841-0.876 μm		

*The MODIS bands of IFOV=500m and 1km are not used in this study.

4. SAMPLE AREA SELECTION

Since the spatial resolution of satellite passive microwave radiometers are rather low as shown on Table 1, it is difficult to identify ice types from the images. Under the cloud free condition, we can identify detailed conditions of sea ice from the images taken by the high resolution optical sensors, such as MODIS, onboard satellites. Figure 2 show the comparison of simultaneously collected AMSR2 ice concentration image and MODIS image of the Bering Sea and the Gulf of St. Lawrence. The AMSR2 ice concentrations were derive using AMSR Bootstrap Algorithm (Comiso, 2009). From the AMSR2 ice concentration images (Figure 2(a) and 3(b)), we can see the clear distribution of sea ice in the Bering Sea and the Gulf of St. Lawrence. However, it is difficult to identify ice thickness differences or thin ice areas from the images. On the other hand, in the MODIS image of Figure 2(b) and 3(b), more detailed sea ice distributions can be observed. Basically, the albedo increases as the ice thickness increases. Through the comparison of the in situ ice thickness measurements with data collected by optical sensor on board satellites, the authors have verified that under the less snow cover and cloud free condition, thin sea ice areas, where the ice thicknesses are around or less than 20cm to 30cm, can be identified in MODIS images (Cho et. al., 2012). In this study, the color composite images of MODIS (Band 1 to blue and red, Band 2 to green) were used for selecting sample areas of thin sea ice, big ice floe, open water and mixed sea ice. In thick ice area, since the albedo of both Band 1 and 2 are high, the area appears in white in the color composite image of MODIS. However, in thin ice area, since the surface and around of thin ice are rather wet, the albedo of Band 2(near infrared) become lower compared with that of Band 1(visible). As a result, most of the thin ice areas appear in purple in the color composite image as sown on Figure 2(b) and 3(b). In this study, the authors defined these dark purple sea ice areas in the MODIS images as thin ice areas.

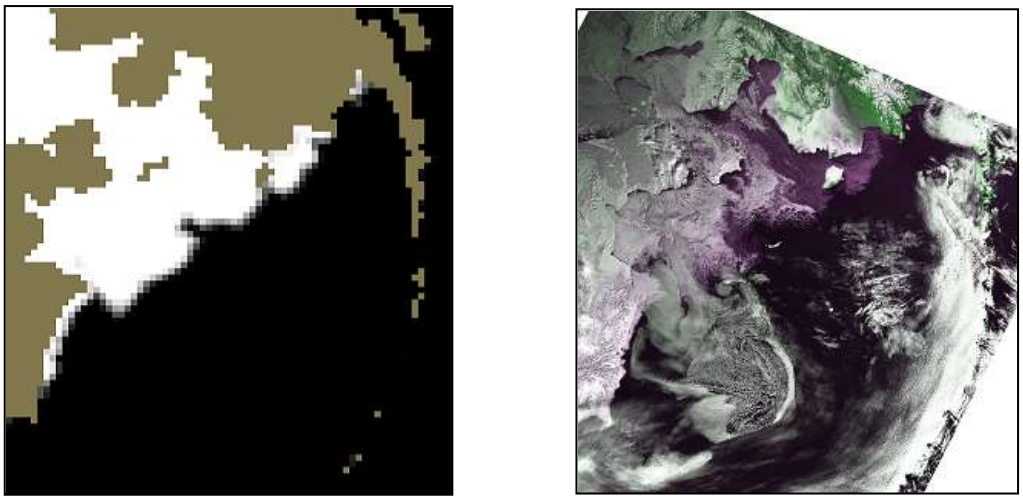

(a) AMSR2 ice concentration image (b) MODIS image

Figure 2. Comparison of AMSR2 and MODIS images. (Bering Sea, February 10, 2014)

(a) AMSR2 ice concentration image (b) MODIS image

Figure 3. Comparison of AMSR2 and MODIS images. (Gulf of St. Lawrence, March 1, 2015)

In order to examine the microwave brightness temperature characteristics of big ice floe, thin ice, mixed ice, and open water, the sample area of each item was selected in the MODIS images of the Bering Sea and the Gulf of St. Lawrence as shown on Figure 4(a) and figure 6(a). Then, the sample areas were overlaid on the AMSR2 image and the AMSR2 brightness temperature data of the sample areas were extracted as shown on Figure 4(b) and figure 6(b). Figure 5 and figure 6 shows the enlarged MODIS image of each sample area.

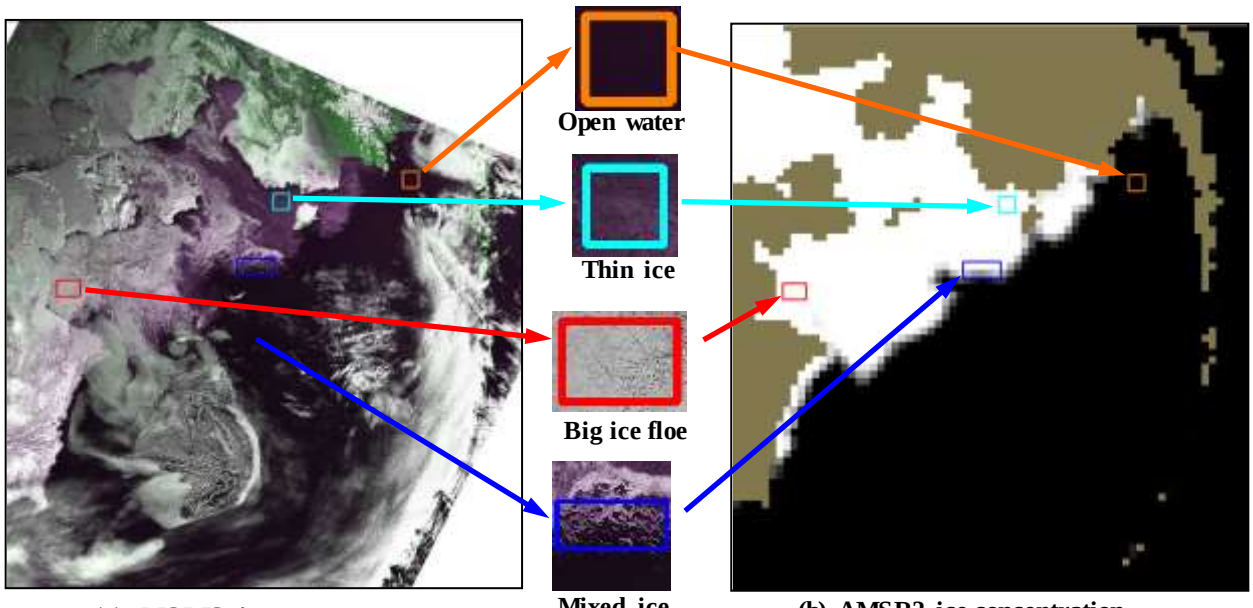

(a) MODIS image (b) AMSR2 ice concentration

Figure 4. Selection of sample areas using MODIS and AMSR2 images. (Bering Sea, February 10,2014)

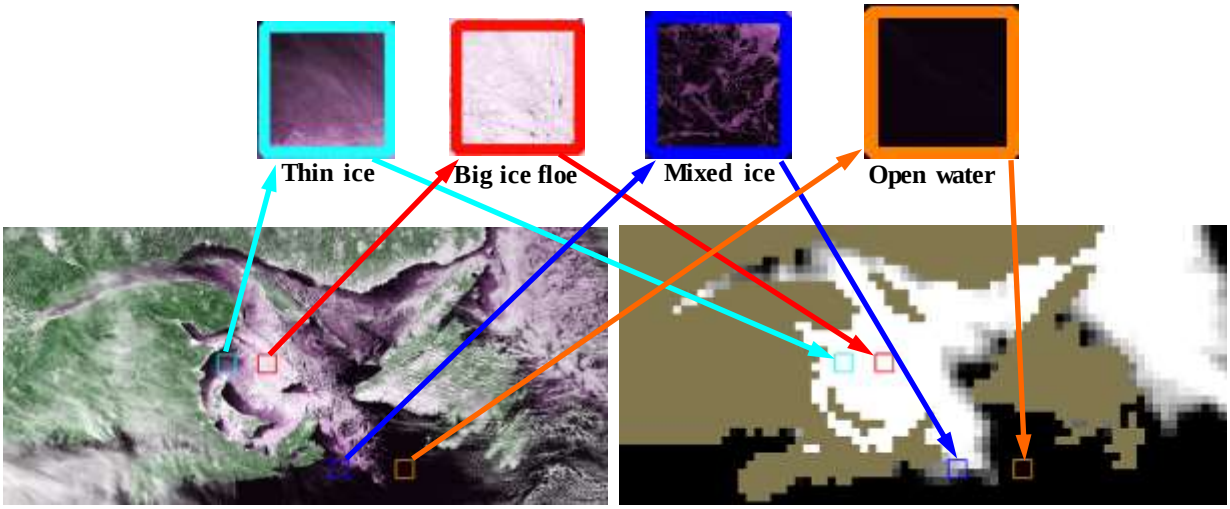

(a) MODIS image **(b) AMSR2 ice concentration**

Figure 5. Selection of sample areas using MODIS and AMSR2 images. (Gulf of St. Lawrence, March 1, 2015)

5. THIN ICE AREA EXTRACTION ALGORITHM

Figure 6 shows the scatter plot of AMSR2 19GHz V versus 19GHz (V-H) of the Bering Sea observed on February10, 2014. In this scatter plot, ● represents open water, ▲ represents mixed ice, ◆ represents thin ice, and ■ represents big ice floe. In our thin ice algorithm, firstly we used the following equation to extract sea ice area with 80% or higher sea ice concentration.

$$(Tb19GHzV) > 245K \quad (1)$$

where Tb19GHzV: Brightness temperature of AMSR2 19GHz V polarization

In low ice concentration sea ice area, various thickness sea ice and open water are mixed within one footprint area of a passive microwave radiometer. One cannot identify the ice thickness of the area. So, in this study, the thin ice areas are only extracted within high ice concentration areas. The microwave brightness temperature of water is much lower in H polarization than in that of V polarization. As explained in chapter 4, thin ice areas are rather wet. Therefore, in thin ice areas, the microwave brightness temperature of thin ice areas become much lower in H polarization than in that of V polarization. While the microwave brightness temperature of consolidated ice does not show big difference between V and H polarization. Considering these characteristics, the authors have introduced the following equation to differentiate thin ice area from consolidated ice.

$$(Tb19GHzV - Tb19GHzH) > -Tb19GHzV + 300K \quad (2)$$

where Tb19GHzH: Brightness temperature of AMSR2 19GHz H polarization

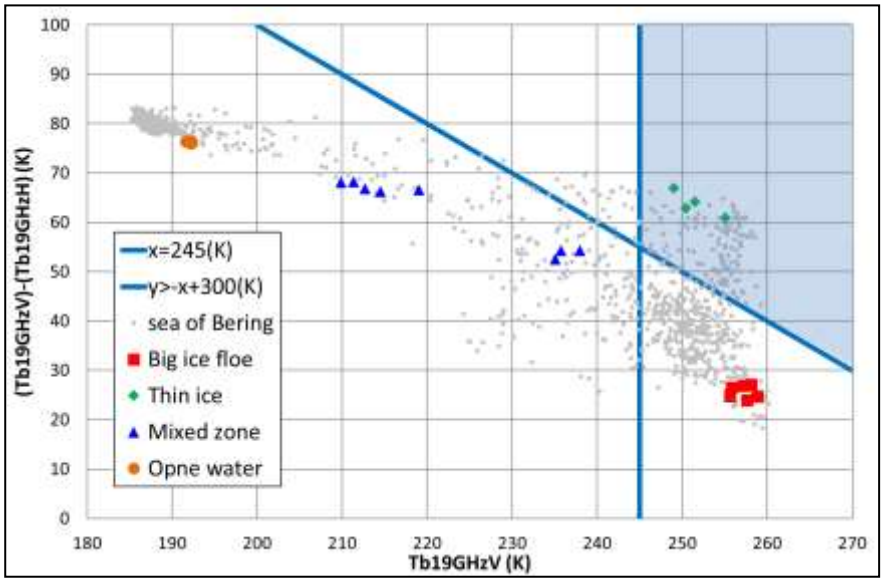

Figure 6. Scatter plots of (19GHzV – 19GHzH) Vs 19GHzV polarization (Bering Sea, February 10, 2014)

Since the brightness temperature difference between V and H polarization is much bigger for thin ice than for big ice floe, extraction of thin ice area can be expected with equation (1) and (2). The parameters of the both equations were specified for the Sea of Okhotsk (Cho et. Al, 2012, Tokutsu et. Al, 2014). However, the distribution of the data of the Bering Sea observed on February 10, 2014 suggests that the algorithm can also be applied to the Bering Sea without changing the equation parameters. Figure 7 show the scatter plot of AMSR2 19GHz V versus 19GHz (V-H) of the Gulf of St. Lawrence observed on March 1, 2015. The distribution of the data also suggests the possibility of applying the same algorithm to the Gulf of St. Lawrence

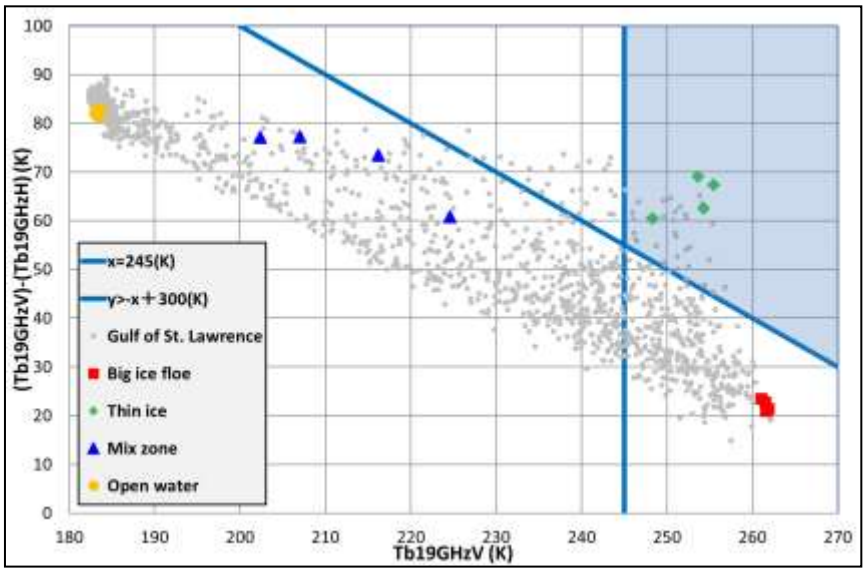

Figure 7. Scatter plots of (19GHzV – 19GHzH) Vs 19GHzV polarization (Gulf of St. Lawrence, March 1, 2015)

6. EXTRACTED RESULT

The authors have applied the thin ice area extraction algorithm to AMSR2 data of the Bering Sea and the Gulf of St. Lawrence. Figure 8(a) show the extracted thin ice areas overlaid on the AMSR2 sea ice concentration image of the Bering Sea observed on February 10, 2014. Figure 8(b) show the extracted thin ice areas overlaid on the MODIS image of the Bering Sea observed on the same day. Figure 9 show the thin ice area extraction result of the Gulf of St. Lawrence for March 1, 2015. Both results show that not all but most of the thin ice areas which are appearing in dark purple in the MODIS images are extracted with the proposed method.

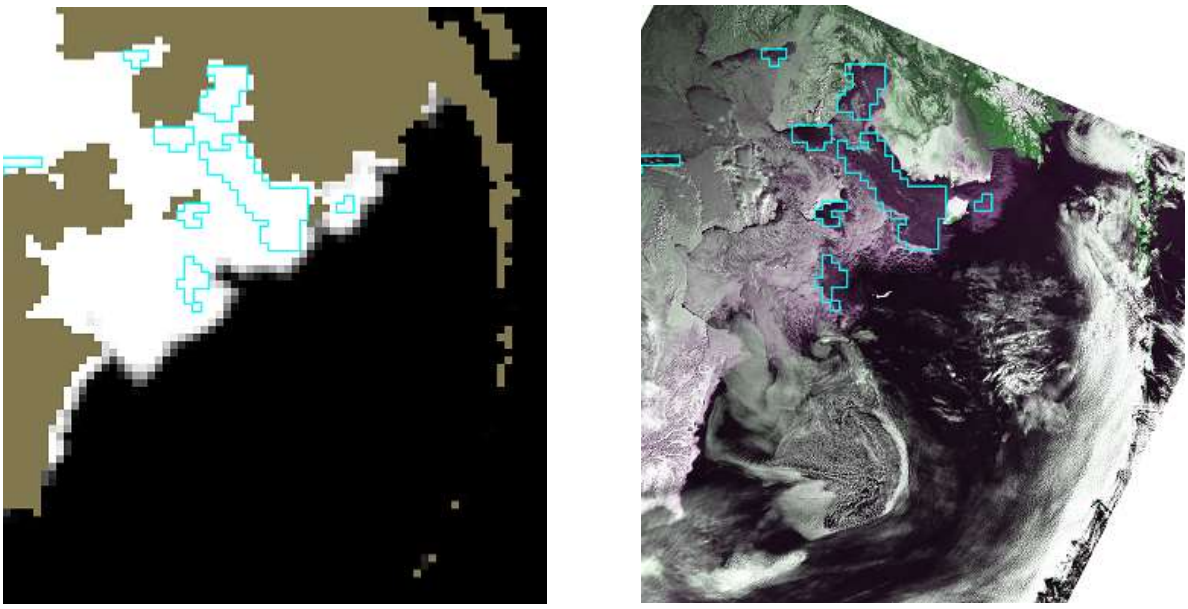

(a)AMSR2 image **(b) MODIS image**

Figure 8. Thin ice area extraction result (Cyan: extracted area) (Bering Sea, February 10, 2014)

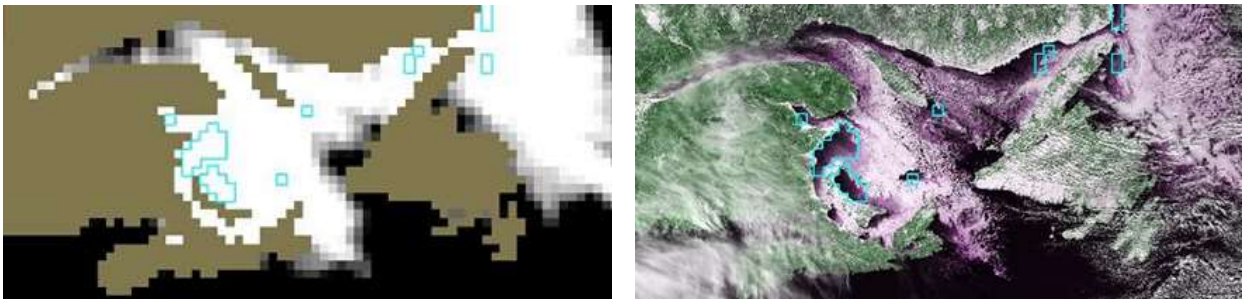

(a)AMSR2 image **(b) MODIS image**

Figure 9. Thin ice area extraction result (Cyan: extracted area) (Gulf of St. Lawrence, March 1, 2015)

7. CONCLUSIONS

In this study, authors have applied the AMSR2 thin ice area extraction algorithm (Cho et. Al, 2012) which was developed for the Sea of Okhotsk to the Bering Sea and the Gulf of St. Laurence. The extracted thin sea ice areas were validated by comparing with simultaneously collected MODIS images. The authors have analyzed total of six scenes for the Bering Sea and four scenes for the Gulf of St. Laurence. The most of the thin ice areas identified in MODIS images were well extracted from AMSR2 data by applying our method. The result suggests the possibility of expanding the algorithm applicable to the seasonal sea ice zones of the Northern Hemisphere. However, it should be noted that the thin ice areas were extracted only for the areas where the sea ice concentration were higher than around 80% in this algorithm. Also, the definition of "thin ice" in this study is the thin ice areas which can be identified in MODIS images by image interpretation.

ACKNOWLEDGEMENT

This study was supported by JAXA under the framework of GCOM-W Project. The authors would like to thank JAXA for their kind support.

REFERENCES

Comiso, J., 2012, Large Decadal Decline of the Arctic Multiyear Ice Cover, Journal of Climate, Vol. 25, pp.1176-1193.

IPCC. 2014. "Summary for Policymakers." *In Climate Change 2013: The Physical Basis*. Contribution of Working Group I to the Fifth Assessment Report of the Intergovernmental Panel on Climate Change, edited by T.F. Stocker, D. Qin, G.K. Plattner, *et al*., Cambridge: Cambridge University Press.

Cavalieri, D. J. and P. Gloersen, 1984, Determination of sea ice parameters with the NIMBUS 7 SMMR, J. Geophys. Res., Vol.89, pp.5355-5369.

Comiso, J. C., 1995 ,SSM/I Sea Ice Concentrations Using the Bootstrap Algorithm", NASA Reference Publication 1380, Maryland, NASA Center for AeroSpace Information.

Tateyama K., H. Enomoto,, T. Toyota. and S. Uto, 2002, Sea ice thickness estimated from passive microwave radiometers, Polar Meteorol. Glaciol., National Institute of Polar Research, Vol. 16, pp.15-31.

Martin S. and R. Drucker, 2005, Improvements in the estimates of ice thickness and production in the Chukchi Sea polynyas derived from AMSR-E, GRL, Vol. 32, L05505

Tamura T., K. I. Ohshima, T. Markus, D. J. Cavalieri, S. Nihashi, N. Hirasawa, 2007, Estimation of Thin Ice Thickness and Detection of Fast Ice from SSM/I Data in the Antarctic Ocean, Journal of Atmospheric and Oceanic Technology, Vol. 24, pp.1757-1772.

Cho, K., Y. Mochizuki, Y. Yoshida, 2012, Thin ice area extraction using AMSR-E data in the Sea of Okhotsk, Proceedings of the 33rd Asian Conference on Remote Sensing, TS-E6-3, pp.1-6.

Tokutsu Y., K. Cho, 2014, Thin Ice Area Extraction Algorithm Using AMSR2 Data for the Sea of Okhotsk, Proceedings of the 35th Asian Conferenceon Remote Sensing, OS-101, pp.1-6.

Cho K., Y. Mochizuki, Y. Yoshida, H. Shimoda and C. F. CHEN, 2012, A study on extracting thin sea ice area from space, International Archives of the Photogrammetry, Remote Sensing and Spatial Information Sciences, Vol. XXXIX-B8, pp.561-566.

Comiso, J. C., 2009, Enhanced Sea Ice Concentrations and Ice Extent from AMSR-E Data, Journal of the Remote Sensing Society of Japan, Vol.29, No.1, pp.199-215.